Chinese Chemical Letters 36 (2025) 109883

Contents lists available at ScienceDirect

Chinese Chemical Letters

journal homepage: www.elsevier.com/locate/cclet

A non-fluorinated liquid-like membrane with excellent anti-scaling performance for membrane distillation

Jianwen Zhao[a,b], Shuai Wang[a,b], Shanshan Zhao[c,*], Liwei Chen[a,b,*], Fangang Meng[c], Xuelin Tian[a,b,*]

[a] State Key Laboratory of Optoelectronic Materials and Technologies, School of Materials Science and Engineering, Sun Yat-sen University, Guangzhou 510006, China
[b] Key Laboratory for Polymeric Composite & Functional Materials of Ministry of Education, Guangzhou Key Laboratory of Flexible Electronic Materials and Wearable Devices, Sun Yat-sen University, Guangzhou 510006, China
[c] Guangdong Provincial Key Laboratory of Environmental Pollution Control and Remediation Technology, School of Environmental Science and Engineering, Sun Yat-sen University, Guangzhou 510006, China

ARTICLE INFO

Article history:
Received 27 January 2024
Revised 2 April 2024
Accepted 10 April 2024
Available online 11 April 2024

Keywords:
Surface modification
Liquid-like membranes
Anti-scaling
Non-fluorinated
Direct contact membrane distillation

ABSTRACT

Membrane distillation (MD) has gained extensive attention for treating highly saline wastewater. However, membrane scaling during the MD process has hindered the rapid development of this technology. Current approaches to mitigate scaling in membrane distillation focus primarily on achieving enhanced hydrophobicity and even superhydrophobicity *via* utilizing fluorinated fibrous membrane or introducing perfluorosilane modification. Considering the environmental hazards posed by fluorinated compounds, it is highly desirable to develop non-fluorinated membranes with enhanced anti-scaling properties for effective membrane distillation. In this study, we present a non-fluorinated liquid-like MD membrane with exceptional anti-scaling performance. This membrane was facilely fabricated by grafting linear polydimethylsiloxane (LPDMS) onto a hydrophilic polyether sulfone (PES) membrane pre-coated with the intermediate layers of polydopamine and silica (denoted as LPDMS-PES). Remarkably, LPDMS-PES manifested a drastically improved scaling resistance in continuous MD tests than its perfluorinated counterpart, *i.e.*, 1*H*,1*H*,2*H*,2*H*-perfluorooctyltrichlorosilane-modified PES membrane (PFOS-PES), in both heterogeneous nucleation-dominated and crystal deposition-dominated scaling processes, despite the latter having a smaller surface energy. LPDMS-PES demonstrated a reduction of crystal accumulation of approximately 85% for NaCl and 73% for $CaSO_4$ in the heterogeneous nucleation-dominated scaling process compared to PFOS-PES. Additionally, in the crystal deposition-dominated scaling process LPDMS-PES exhibited a reduction of about 70% in scale accumulation. These results explicitly evidenced the great potential of the liquid-like membrane to minimize scaling in membrane distillation by inhibiting both scale nucleation and adhesion onto the membrane. We believe the findings of this study have important implications for the design of high-performance MD membranes, particularly in the quest for environmentally sustainable alternatives to perfluorinated materials.

To address the global challenge of water scarcity, membrane separation technology has been widely used for seawater desalination [1–3] and wastewater reclamation [4–6] to acquire freshwater resources. MD is a desalination process that relies on thermal driving and hydrophobic membranes, and has gained extensive attention for treating highly saline wastewater [7]. Compared to conventional nanofiltration and reverse osmosis desalination techniques, MD exhibits lower sensitivity to salinity. Another crucial advantage of MD is its ability to utilize low-grade waste heat [8,9], thereby improving energy efficiency, which is of profound significance for global carbon reduction. However, conventional hydrophobic membranes in the MD desalination process often encounter challenges related to scaling, which hinder the rapid progress and industrialization of MD technology [10,11]. The presence of scaling layers not only increases the resistance to heat and mass transfer, but also leads to pore blockage, thereby reducing membrane permeability. Additionally, scaling layers can decrease the surface hydrophobicity of the membrane, resulting in membrane wetting and subsequent salt leakage [12,13].

* Corresponding authors.
E-mail addresses: zhaoshsh7@mail.sysu.edu.cn (S. Zhao), chenlw28@mail.sysu.edu.cn (L. Chen), tianxuelin@mail.sysu.edu.cn (X. Tian).

https://doi.org/10.1016/j.cclet.2024.109883
1001-8417/

In the MD process, scaling occurs primarily through two pathways: heterogeneous nucleation (followed by growth) of scale crystals on the membranes surface, and crystalline deposition from the solution onto the membrane surface [14]. In recent years, extensive research has been conducted to explore superhydrophobic surfaces (water contact angle $> 150°$) for anti-scaling purposes due to their surface air layer, high energy barrier for nucleation and enhanced interface slippage [15–18]. However, the preparation processes for superhydrophobic surfaces are complex and often involve the use of expensive fluorosilanes, which could lead to the formation of environmentally detrimental carcinogens [19,20]. Additionally, the fine micro- and nanostructures required by superhydrophobicity raise concerns on the durability issue. Furthermore, many existing studies have primarily focused on heterogeneous nucleation on membrane surfaces, neglecting the influence of crystal deposition from the solution on membrane scaling [1]. Therefore, it is essential to explore an easy-to-prepare and non-fluorinated MD membrane that can simultaneously resist heterogeneous nucleation and crystal deposition.

Coatings composed of highly flexible molecular brushes, such as polymer brushes with extremely low glass transition temperature (T_g) down to $-100\,°C$, can impart a surface with liquid-like properties [21,22]. While one end of the molecular brush is fixed onto the substrate, the rest part is highly mobile and free to move at room temperature due to the extremely low T_g of the polymer, exhibiting highly mobile characteristics. These mobile brushes can thus function as a highly slippery liquid-like layer, thereby reducing the interface interaction with both liquids and solids. Such coatings have attracted increasing attention in recent years and are being explored for anti-scaling purposes on porous membrane surfaces. Huang *et al.* investigated on the MD performance of polyvinylidene fluoride (PVDF) membranes modified with different perfluorosilanes. They found that the membrane coated with a perfluorosilane containing a single hydrolysis site possessed superior anti-scaling property compared to the membrane coated with a perfluorosilane containing triple hydrolysis sites. They attributed this interesting finding to the liquid-like nature of the former coating [23]. However, the perfluorosilane (*i.e.*, 1*H*,1*H*,2*H*,2*H*-perfluorodecyltrimethoxysilane) employed in their study is not a typical liquid-like molecule and the use of perfluorosilanes in the preparation raises ongoing concerns about environmental pollution. In comparison, fluorine-free linear polydimethylsiloxane (LPDMS) can serve as a more favorable alternative. This biocompatible compound is characterized by its remarkable flexibility with T_g as low as $-127\,°C$, enabling it to exhibit excellent liquid-like property. Grafting LPDMS onto porous membranes has been demonstrated to significantly enhance the surface's ability to resist fouling caused by viscous oily substances [24]. However, in the current field of MD, the existing references to PDMS predominantly refer to crosslinked PDMS, primarily serving the functions of adhesion and hydrophobicity enhancement [16,25,26]. Although a recent report by Liu *et al.* showcased an superhydrophobic LPDMS/TiO_2/PVDF composite membrane with enhanced anti-scaling and anti-wetting properties [27], they attributed these properties to the membrane's slippery surface and superhydrophobicity, without emphasizing the crucial role of the flexible molecular chains. Overall, there has been limited attention paid to the impact of the flexible chains of LPDMS on the anti-scaling performance of MD membranes. Furthermore, the existing MD membranes are either made of fluoropolymers or surface-functionalized with fluorosilanes. There is still a lack of completely fluorine-free MD membranes that can effectively resist scaling.

In this study, a fully fluorine-free MD membrane featuring liquid-like surface chemistry was prepared. The membrane, named LPDMS-PES, was created by covalently grafting LPDMS chains onto a polyethersulfone (PES) matrix membrane that had been pre-coated with polydopamine (PDA) and silica (SiO_2). To identify the crucial influence of molecular chain flexibility on the anti-scaling properties, relatively rigid 1*H*,1*H*,2*H*,2*H*-perfluorooctyltrichlorosilane (PFOS) chains were grafted onto the matrix membrane as a comparative sample (PFOS-PES). The results show that LPDMS-PES exhibited a markedly enhanced resistance to scaling in continuous MD processes compared to its perfluorinated counterpart in both heterogeneous nucleation-dominated and crystal deposition-dominated scaling tests and effectively delayed the occurrence of scaling-induced wetting issues on the membrane. The anti-scaling mechanism of LPDMS-PES is analyzed in detail. On one hand, the highly mobile LPDMS brushes are speculated to restrict the ion-surface interaction and inhibit the aggregation of ions on the membrane surface, thereby delaying heterogeneous nucleation of salt crystals. On the other hand, the slippery LPDMS layer greatly reduces surface adhesion to solids, hindering deposition of crystals onto the membrane surface.

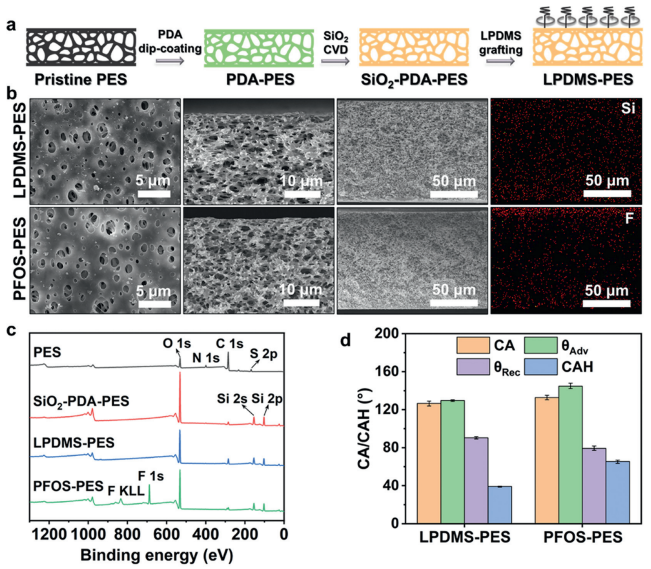

Fig. 1. (a) Schematic illustration of the preparation process of LPDMS-PES. (b) SEM images of the top and cross-section views of LPDMS-PES and PFOS-PES, and the corresponding element mappings of the two membranes. (c) XPS spectra, and (d) water contact angle (CA), advancing contact angle (θ_{Adv}), receding contact angle (θ_{Rec}) and contact angle hysteresis (CAH) of the two membranes.

LPDMS-PES and the comparative PFOS-PES membrane were prepared through stepwise surface modification of commercially available PES membranes. Firstly, a PDA layer and a SiO_2 layer were sequentially coated onto the membrane surface. Subsequently, after surface hydroxylation, LPDMS or PFOS were grafted onto the surfaces of the membranes, as depicted in Fig. 1a. The morphologies of the pristine PES membrane and the membranes after intermediate modification steps were examined using FE-SEM analysis. The impact of the PDA layer on the morphology of membrane pores was minimal, as shown in Fig. S1 (Supporting information), which was consistent with previous reports [28]. The cross-sectional view images revealed that the deposition of SiO_2 did not cause blockages within the interior of the SiO_2-PDA-PES membrane. The EDS analyses confirmed the successful deposition of PDA and SiO_2 onto the membranes (Fig. S2 in Supporting information). The SEM images of LPDMS-PES and PFOS-PES (Fig. 1b) indicated that their morphologies closely resembled that of the SiO_2-PDA-PES membrane. The thickness of the grafted molecular layer can be considered negligible. According to previous reports, the thickness of the LPDMS coating was approximately 4 nm [29]. Hence, the influence of all surface modifications on the structures of the membrane pores can be disregarded.

It is well known that the abundant amino groups and hydroxyl groups presented on PDA contribute to its strong adhesion nature [30,31], allowing it to adhere well to various substrates or substances. The PDA layer can thus promote the binding of SiO_2 to the PES matrix membrane. Additionally, rich hydroxyl groups can be created on the surface of SiO_2 by oxygen plasma treatment, and the presence of Si-OH bonds facilitates the reaction with trimethoxysilane-terminated PDMS for grafting the liquid-like layer. To investigate the crucial role of PDA and SiO_2 intermediate layers in the subsequent liquid-like surface chemistry modification, we conducted LPDMS grafting experiments under various conditions. The variables in these experiments were the presence of PDA or SiO_2 layers. The prepared comparative samples included the membrane prepared without pre-coated PDA and SiO_2 layers (sample a), the membranes prepared with only pre-coated PDA layer (samples b and c, oxygen plasma treatment was conducted prior to LPDMS grafting for sample c and not for sample b), and the membrane prepared with only pre-coated SiO_2 layer (sample d). The water contact angles of the above samples are shown in Fig. S3 (Supporting information). The contact angles of all the samples were lower than that of LPDMS-PES, indicating a degraded surface hydrophobicity. Samples b and c, prepared with only pre-coated PDA layer, exhibited high hydrophilicity regardless of oxygen plasma treatment. This suggested a very limited reactivity between the Si-O bonds of LPDMS and the hydroxyl groups of PDA layer. Combining the results in Fig. 1b and Fig. S3, it can be concluded that the SiO_2 layer plays an essential role to ensure effective grafting of LPDMS chains onto the membrane surface. The deposited SiO_2 not only existed in the form of particles but also covered the membrane surface as a thin layer. Additionally, sample d exhibited a contact angle similar to that of sample a, suggesting that in the absence of PDA adhesion layer, SiO_2 cannot effectively deposit onto the membrane surface. Therefore, the presence of both PDA and SiO_2 layers was indispensable for grafting LPDMS onto the membrane surface.

The successful modification of the PES membranes with LPDMS and PFOS was confirmed by XPS and EDS analyses (Figs. 1b and c, Table S1 in Supporting information). The surface roughness of LPDMS-PES and PFOS-PES was examined using AFM, as illustrated in Fig. S4 (Supporting information). Surface roughness is known to play an important role in scaling, with higher roughness increasing scaling possibility [32,33]. The arithmetic average roughness (R_a) values of LPDMS-PES and PFOS-PES were 178.63 and 179.23 nm, respectively, indicating similar roughness between the two membranes. Therefore, the influence of surface roughness on the difference in scaling resistance between LPDMS-PES and PFOS-PES can be disregarded.

Pore size, porosity, and thickness are crucial factors that influence the performance of membrane distillation. To evaluate the effectiveness of the modifications, the structure parameters of the prepared membranes were measured, and the results are presented in Table 1. The presence of the PDA coating and SiO_2 layer in the SiO_2-PDA-PES membrane led to a slight increase in thickness compared to the original PES membrane, accompanying a slight reduction in porosity. LPDMS-PES and PFOS-PES, after grafting modifications, displayed minimal changes in porosity, and thickness compared to SiO_2-PDA-PES. Pore size testing was conducted using a gas-liquid displacement technique. The measurement results and pore size distribution of different membranes are presented in Table S2 and Fig. S5 (Supporting information). Interestingly, LPDMS-PES shows a slightly larger mean pore size than the other membranes. We speculate that the liquid-like nature of the LPDMS coating is responsible for this unusual observation. The highly slippery nature of the LPDMS coating probably facilitates expelling the infiltrated liquid from LPDMS-PES due to the reduced solid-liquid interfacial interaction. Consequently, a smaller gas pressure is sufficient for removing the infiltrated liquid in the gas-liquid displacement measurement, thereby resulting in a slightly increase in the calculated mean pore size. The difference in the actual pore size between LPDMS-PES and the other membranes should be smaller than the calculated results and can be considered negligible. Furthermore, the pure water flux of PFOS-PES is comparable to that of LPDMS-PES, consistent with the porosity result (Fig. S6 in Supporting information). Overall, the surface modifications of the PES membranes had negligible effects on pore size and thickness.

Table 1
LEP, porosity, thickness, and mean pore diameter of membranes.

Membranes	LEP (bar)	Porosity (%)	Thickness (μm)	Mean pore diameter (μm)
Pristine PES	–	77.69	114.2	0.1882
SiO_2-PDA-PES	–	76.36	114.9	0.1844
LPDMS-PES	1.8	75.47	115.0	0.1930
PFOS-PES	2.4	75.81	114.9	0.1840

The wetting properties of LPDMS-PES and PFOS-PES were evaluated using a contact angle instrument, and the results are presented in Fig. 1d. PFOS-PES exhibited a slightly higher static water contact angle compared to LPDMS-PES (132.8° *vs.* 126.5°), suggesting a slightly greater hydrophobicity of the former. However, LPDMS-PES displayed a significantly lower contact angle hysteresis (CAH) than PFOS-PES (39.2° *vs.* 65.5°), indicating reduced resistance to liquid motion on the LPDMS-PES surface. This is a typical characteristic of a liquid-like coating, as the highly flexible LPDMS chains can facilitate the movement of the solid-liquid-gas contact line and thus promote liquid mobility on the surface [22,34].

The liquid entry pressure (LEP) serves as a quantitative metric to measure membrane liquid repellency. Based on the Laplace-Young equation [35], LEP is strongly influenced by the membrane's hydrophobicity and maximum pore size. Specifically, LEP is directly proportional to hydrophobicity and inversely proportional to maximum pore size. In this study, the LEP values were determined to be 1.8 bar for LPDMS-PES and 2.4 bar for PFOS-PES (Table 1), indicating that both membranes were basically capable of operating DCMD tests. The comparable average pore sizes of the two membranes further support the qualitative consistency between the LEP results and the contact angle measurements.

As introduced above, scaling occurs primarily through two pathways: Heterogeneous nucleation and subsequent growth of scale crystals on the membranes surface, and crystalline deposition from the solution onto the membrane surface. To conduct a comprehensive investigation on the anti-scaling behaviors of the LPDMS-PES and PFOS-PES membranes in the DCMD processes, two sets of scaling experiments were designed, including heterogeneous nucleation-dominated scaling experiments and crystal deposition-dominated scaling experiments.

In the heterogeneous nucleation-dominated scaling experiments, DCMD test was first conducted at 60 °C for 80 h using a 0.6 mol/L NaCl solution as the feed. As the employed NaCl concentration was far below its solubility (6.4 mol/L) at this temperature, homogeneous nucleation in the bulk solution was not likely to occur. In contrast, concentration polarization during membrane separation could lead to higher solute concentration and local oversaturation near the membrane surface, thereby inducing heterogenous nucleation and further growth of NaCl crystals on the membrane surface. Fig. 2a shows the membrane distillation results of LDPSM-PES and PFOS-PES when the NaCl solution was used as the feed. Throughout the experiment, the permeate flux of LPDMS-PES remained stable at around 6.4 kg m^{-2} h^{-1}. Moreover, the permeate conductivity was constantly below 9.22 μS/cm,

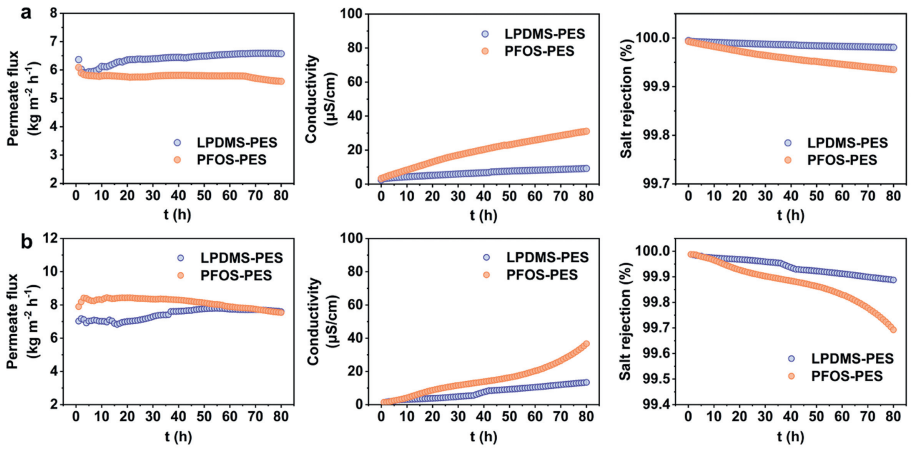

Fig. 2. Membrane distillation performances of LPDMS-PES and PFOS-PES under heterogeneous nucleation-dominated scaling process during DCMD tests. (a) Time-dependent permeate flux, permeate conductivity and salt rejection of the two membranes using a 0.6 mol/L NaCl solution as the feed, and (b) using a solution containing 20 mmol/L $CaCl_2$ and 20 mmol/L Na_2SO_4 (SI = 0.82) as the feed.

and the salt rejection remained above 99.98%, indicating a high-quality permeate water production. Although the permeate flux of PFOS-PES was close to that of LPDMS-PES at the beginning of the DCMD process, it decreased by 8.05% relative to the initial value after 80 h. This reduction can be attributed to the precipitation of NaCl particles which leads to pore blockage. The permeate conductivity for PFOS-PES gradually increased and reached about 31.11 μS/cm after 80 h, approximately 3.37 times that of LPDMS-PES, suggesting partial wetting of the membrane pores due to scale accumulation. Simultaneously, the salt rejection drops to 99.93%, indicating noticeable salt leakage for PFOS-PES. The above facts demonstrate clearly that LPDMS-PES possesses superior membrane distillation performance and anti-scaling ability compared to PFOS-PES.

$CaSO_4$ scale is one of the most insoluble and common scales in seawater and various groundwater sources [28,36]. To further compare the scale resistance of LPDMS-PES and PFOS-PES, DCMD tests were also conducted at 60 °C using a feed solution containing 20 mmol/L $CaCl_2$ and 20 mmol/L Na_2SO_4 to induce gypsum crystal accumulation on the membrane surface. The saturation index (SI) of the solution was 0.82 (SI < 1), and thus only heterogenous nucleation-dominated scaling was expected to occur. While a number of crystals accumulated on the membrane surface of LPDMS-PES after 48 h of testing, none were observed in the feed solution during the same period (Fig. S7a in Supporting information). These facts confirm the dominance of heterogeneous nucleation in this experimental group. As shown in Fig. 2b, the permeate flux of LPDMS-PES remained stable at 7.3 ± 0.5 kg m^{-2} h^{-1} during an 80-hour DCMD test. The permeate-side conductivity was always less than 13.43 μS/cm throughout the test, and the salt rejection rate remained above 99.88%, indicating minimal decline in permeate quality. In comparison, the permeate flux of PFOS-PES after 80 h of operation exhibited a 9.68% reduction relative to the average permeate flux of the initial 40 h. Moreover, the permeate conductivity increased to 2.73 times that of LPDMS-PES, and the salt rejection rate dropped to 99.69%, indicating significant salt leakage. These results further verified the enhanced anti-scaling and membrane distillation performances of LPDMS-PES.

The detailed scaling behaviors of LPDMS-PES and PFOS-PES were investigated using SEM, EDS elemental mapping and gravimetric analyses. After the DCMD test, the membranes were extracted from the membrane module, carefully cleaned and dried, and then subjected to SEM imaging and elemental mapping. The crystallizing results when using the NaCl solution as the feed are shown in Figs. 3a-c. Both SEM imaging and EDS elemental mapping showed that the surface and cross-sections of PFOS-PES contained a substantial amount of NaCl crystals (Fig. 3a). In contrast, the crystals were almost absent on the surface and cross-sections of LPDMS-PES. Fig. 3b shows that, while the membrane pores of LPDMS-PES were free of any crystals, the membrane pores of PFOS-PES membrane were obstructed by NaCl crystals, resulting in reduced flux and salt rejection. Furthermore, gravimetric analyses indicated that the unit area weight gain of LPDMS-PES caused by scaling was reduced by about 85% compared to that of PFOS-PES (Fig. 3c). All these facts demonstrate the remarkably enhanced anti-scaling property of LPDMS-PES compared to PFOS-PES.

The investigation on the scaling behaviors of gypsum crystals on the membranes gave similar results (Figs. 3d-f). As shown in Fig. 3d, though both membrane surfaces displayed needle-like or rod-like gypsum crystals (Fig. S8 in Supporting information), the scaling extent on LPDMS-PES was considerably less. Moreover, according to EDS mapping analyses, the presence of gypsum crystals on the surface of LPDMS-PES did not lead to scaling or wetting of the internal membrane pores. In contrast, the internal pores of PFOS-PES were filled by gypsum, causing deformation of the membrane pores (Fig. 3e). Additionally, LPDMS-PES exhibited a decrease of unit area weight gain by about 73% compared to PFOS-PES (Fig. 3f). Therefore, it can be concluded that the dynamic molecular chains of LPDMS can effectively inhibit heterogeneous nucleation of both NaCl and gypsum on the membrane surface and impart the membrane with significantly enhanced scale resistance.

We further studied the scale resistance of LPDMS-PES and PFOS-PES in crystal deposition-dominated scaling tests (Fig. 4). To examine the anti-scaling ability of the two membranes, a 10-hour DCMD test was conducted using a feed solution containing 50 mmol/L $CaCl_2$ and 50 mmol/L Na_2SO_4. The SI of the solution was as high as 2.43, so that homogeneous nucleation of gypsum in the bulk solution tended to occur. As shown in Fig. 4b, many precipitates began to appear in the solution within 13 min of operation, owing to the homogeneous nucleation and growth of gypsum crystals. In principle, heterogeneous nucleation should also occur on the membrane surfaces due to salt oversaturation. However, it was observed that the direct crystal formation on the membrane surface was limited compared to the substantial crystal formation in the solution, suggesting the dominant role of crystal deposition from the solution onto the membrane in influencing membrane scaling and membrane distillation performances. The crystal size on the membrane surface closely resembled that in the feed solution after 2 h of testing (Fig. S7b in Supporting information),

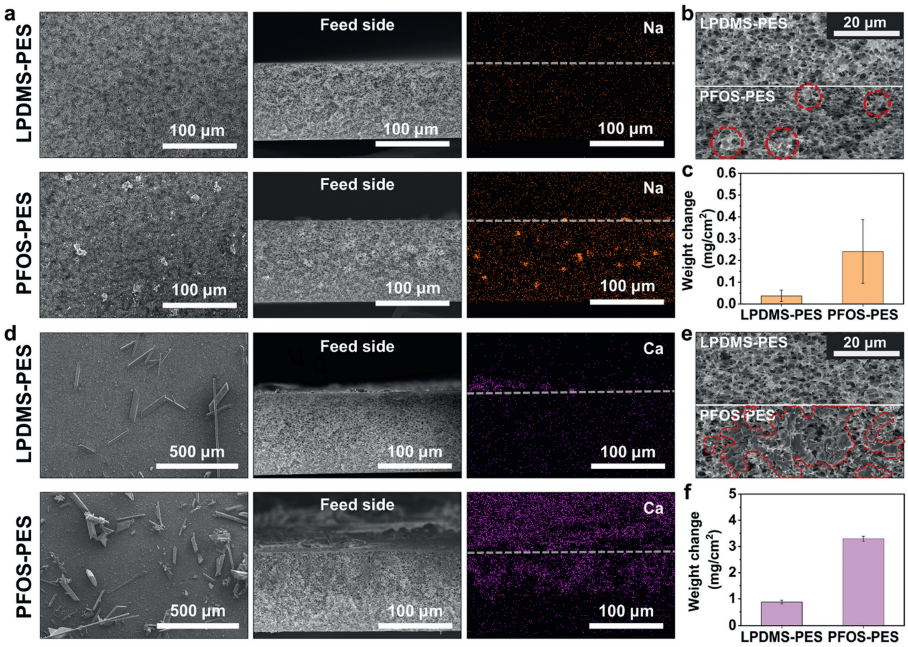

Fig. 3. (a) SEM images and the corresponding cross-section EDS mapping of the membranes after heterogeneous nucleation-dominated scaling tests for 80 h using a 0.6 mol/L NaCl solution as the feed in DCMD, and (b) enlarged cross-section images and (c) scale weigh gain per unit area of the membranes. (d) SEM images and the corresponding cross-section EDS mapping of the membranes after heterogeneous nucleation-dominated scaling tests for 80 h using a solution containing 20 mmol/L $CaCl_2$ and 20 mmol/L Na_2SO_4 as the feed, and (e) enlarged cross-section images and (f) scale weigh gain per unit area of the membranes. The presence of NaCl and gypsum crystals on the PFOS-PES membrane is highlighted by the red dotted line in (b) and (e), respectively.

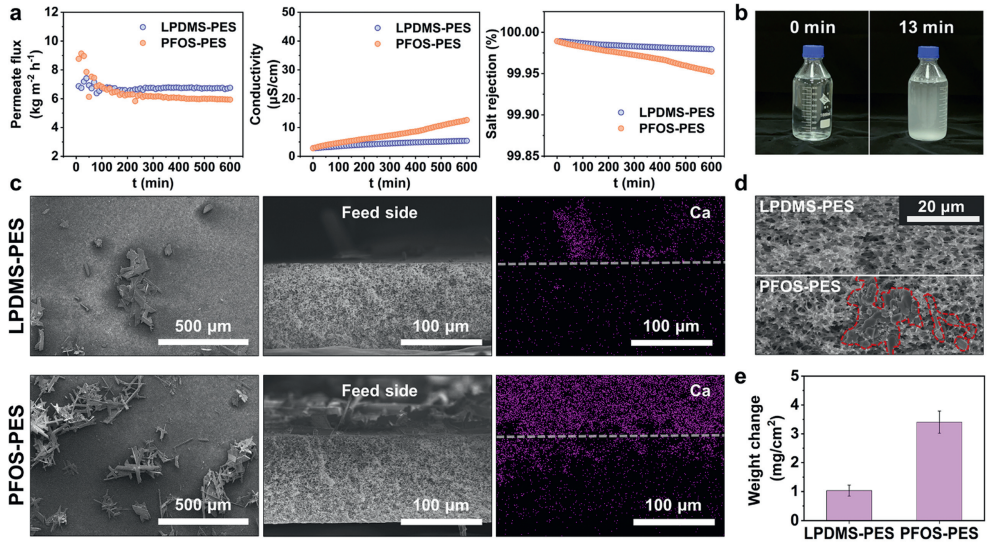

Fig. 4. Membrane distillation performance of LPDMS-PES and PFOS-PES under crystal deposition-dominated scaling process during DCMD tests. (a) Time-dependent permeate flux, permeate conductivity and salt rejection of the two membranes using a solution containing 50 mmol/L $CaCl_2$ and 50 mmol/L Na_2SO_4 (SI = 2.43) as the feed. (b) Evolution of the feed solution over time during DCMD tests. (c) SEM image and the corresponding cross-section EDS mapping of the membranes after 10 h DCMD tests. (d) Enlarged cross-section images and (e) scale weigh gain per unit area of the membranes. The presence of gypsum crystals on PFOS-PES is highlighted by the red dotted line in (d).

and moreover, the crystal size was larger than those observed in the heterogeneous nucleation-dominated scaling experiment. All these facts suggest that the crystals deposited on the membrane surface are predominantly derived from the solution rather than heterogeneous nucleation. As depicted in Fig. 4a, LPDMS-PES could maintain a stable permeate flux of 6.9 ± 0.5 kg m^{-2} h^{-1} within a 10-h DCMD process, suggesting minimal scaling and wetting of the membrane. Simultaneously, the permeate conductivity remained constantly below 5.41 μS/cm, indicating the inexistence of salt leakage. In contrast, the permeate flux for PFOS-PES decreased by 31.8% relative to the maximum value within the initial 190 min of the DCMD test. The decline in the permeate flux was accompanied by an increase in the permeate conductivity and a decrease in the salt rejection, suggesting rapid accumulation of gypsum onto the membrane surface which consequently induced membrane wetting and salt leakage. SEM and EDS elemental mapping analyses further revealed the difference in scale resistance between the two membranes. While a small amount of gypsum crystals was present on the surface of LPDMS-PES, substantial crystal attachment was observed on the surface of PFOS-PES (Fig.

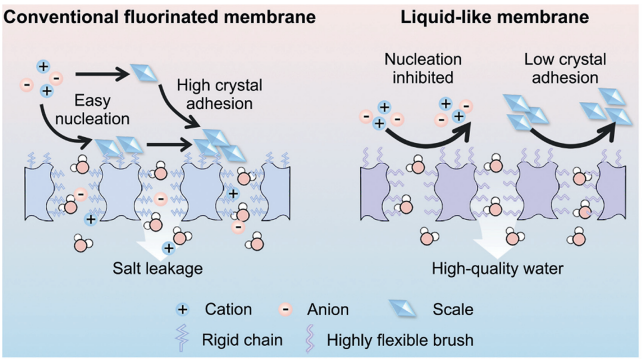

Fig. 5. Schematics illustration of the anti-scaling mechanisms of the MD membrane featuring liquid-like surface chemistry. Compared to conventional fluorinated membranes with relatively rigid fluorocarbon chains, the highly mobile molecular chains on the surface of the liquid-like membrane can better inhibit both heterogeneous nucleation and crystal deposition on the membrane surface, thereby imparting the membrane with excellent anti-scaling performance.

4c). Notably, the inner pores of PFOS-PES were also found to be severely contaminated by gypsum crystals (Fig. 4d). This can be attributed to the scale deposition-induced wetting of the membrane pores, which facilitated the gradual penetration of the feed solution into the membrane and the subsequent accumulation of gypsum crystals in the inner pores. In contrast, LPDMS-PES not only showed greatly reduced gypsum scale on the surface, but also was almost free of scale in the inner pores. The unit area scale weight gain of LPDMS-PES showed a reduction of about 70% compared to that of PFOS-PES (Fig. 4e), indicating a significantly lower scale adhesion of LPDMS-PES relative to PFOS-PES.

Clearly, LPDMS-PES manifests a drastically enhanced ability to inhibit both the heterogeneous nucleation of scale crystals on the membrane surface and the deposition and adhesion of crystals from the solution compared to PFOS-PES (Fig. S9 in Supporting information). We calculated the surface energy of the LPDMS and PFOS coatings, and the former exhibited a lower surface energy than the latter (22.14 *vs.* 8.76 mN/m, Table S3 in Supporting information for details). Since the LPDMS coating exhibits a smaller contact angle and higher surface energy compared to the PFOS coating, the difference in scale resistance between LPDMS-PES and PFOS-PES cannot be explained by merely considering the influence of surface energy. The liquid-like nature of the LPDMS brushes should play a unique role, contributing to the enhanced anti-scaling ability of LPDMS-PES due to the nucleation inhibition ability of the dynamic LPDMS molecular chains and their low adhesion characteristics (Fig. 5).

When heterogeneous nucleation on the membrane surface is dominant during the DCMD process, the superior anti-scaling performance of the LPDMS-PES cannot be well explained by classical nucleation theory. According to classical nucleation theory, the relationship between the heterogeneous nucleation energy barrier (ΔG^*_{het}) and the homogeneous nucleation energy barrier (ΔG^*_{hom}) on the membrane surface can be expressed as [37]:

$$\frac{\Delta G^*_{het}}{\Delta G^*_{hom}} = \frac{1}{4}\left(2+cos\theta_{lcm}\right)\left(1-cos\theta_{lcm}\right)^2\left[1-\varepsilon\frac{(1+\cos\theta_{lcm})^2}{(1-\cos\theta_{lcm})^2}\right]^3 \quad (1)$$

where θ_{lcm} represents the contact angle of crystal on the membrane surface in the solution environment, and ε denotes the membrane surface porosity. Typically, the contact angle of a liquid on the membrane surface in the air (θ_{glm}) is more readily obtained through experimental measurement. Previous studies have shown that the trend of $\Delta G^*_{het}/\Delta G^*_{hom}$ calculated using θ_{glm} or θ_{lcm} is similar [38]. Therefore, for a qualitative comparison, we used θ_{glm} instead of θ_{lcm} to perform the theoretical calculation, and the results are presented in Table S4 (Supporting information). Considering the similar membrane surface porosities of the two samples, the LPDMS-PES surface with lower hydrophobicity exhibited a lower nucleation energy barrier. This suggested, in principle, more scaling tend to occur on LPDMS-PES. However, the experimental results were contrary to theoretical prediction, indicating that the classical nucleation theory is not applicable to understanding the nucleation events on the LPDMS-PES surface [38].

To validate the influence of molecular chain mobility on anti-scaling performance, $CaSO_4$ scaling tests were conducted using the setup shown in Fig. S10a (Supporting information). Beakers were modified with LPDMS, crosslinked PDMS (CPDMS) and PFOS respectively, followed by the addition of 25 mL of 100 mmol/L $CaCl_2$ and 25 mL of 100 mmol/L Na_2SO_4. The mixture was stirred at 35 °C to achieve $CaSO_4$ supersaturation. The conductivity of the solution was continuously measured to monitor the nucleation and growth of $CaSO_4$ crystals as they precipitated. Since the energy barrier for heterogeneous nucleation is much lower than that for homogeneous nucleation, crystals tend to form on the walls of the beaker. Therefore, a coating that inhibits heterogeneous nucleation can lead to a slower decrease in the conductivity of the solution. The experimental results, as depicted in Fig. S10b (Supporting information), demonstrate the LPDMS-coated beaker exhibited the slowest rate of conductivity decline. This suggests that the highly flexible LPDMS brush coating significantly delays heterogeneous nucleation in the beaker compared to the CPDMS and PFOS coatings. Considering the relatively rigid molecular chains of the PFOS coating and the restricted molecular chain movement the CPDMS coating, the above facts imply the significance of molecular chain mobility in inhibiting heterogeneous nucleation.

The superior anti-scaling performance of the LPDMS-PES surface in terms of inhibiting heterogeneous nucleation can thus be attributed to the liquid-like nature of the highly mobile LPDMS molecular chains. Heterogeneous nucleation of salt crystals involves aggregation and orderly arrangement of cations and anions on the membrane surface. We speculate that the molecular chains of LPDMS may impede heterogeneous nucleation of salt crystals for the following reasons. Due to its extremely low glass transition temperature, LPDMS exhibits high mobility at room temperature. While one end of the LPDMS chain is grafted onto the membrane surface, the other end can continuously rotate and move [21,39]. The highly mobile nanoscale molecular chains hinder the orderly aggregation of cations and anions on the surface, consequently delaying the heterogenous nucleation of salt crystals. In the case of PFOS-PES, the less mobile PFOS molecular chains are quite sluggish, resulting in a relatively rigid surface layer. This rigidity makes it easier for ions to aggregate and initiate nucleation on the surface (Fig. S10 in Supporting information).

In addition, it was recently proposed that on highly slippery surfaces with a substantial slip length, the continuous movement of the interface restricts the interaction between the liquid and the membrane surface, thereby suppressing surface nucleation as well as crystal adhesion [40,41]. Our earlier investigations have shown that the liquid-like coating can behave as a lubrication layer and lead to increased slip lengths [42]. Therefore, we can expect that the liquid-like LPDMS layer to promote liquid slip on the membrane surface [43]. This enhanced interface slip could restrict the interaction between the solution and the membrane surface, further inhibiting nucleation of salt crystals on the surface. Overall, the probability for the occurrence of heterogeneous nucleation on the liquid-like surface is greatly reduced compared to that on the perfluorinated surface even the latter has a lower surface energy.

In the case that crystal deposition from the solution onto the membrane surface is the main source of surface scaling, the liquid-like LPDMS chains are also superior to the relatively

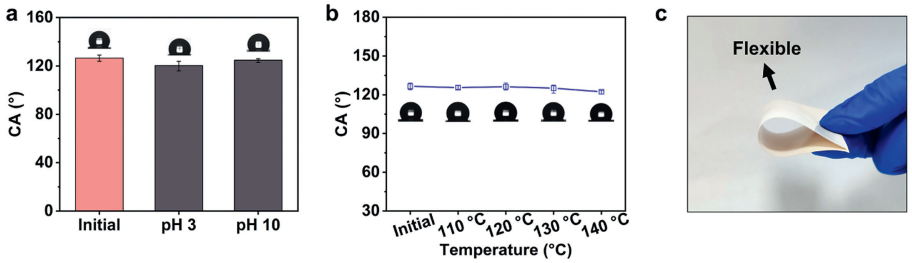

Fig. 6. (a) Alterations in the water contact angle of LPDMS-PES after immersing it in hydrochloric acid solution (pH 3) and sodium hydroxide solution (pH 10) for 2 h, respectively. (b) Alterations in the water contact angle of LPDMS-PES after heating it at different temperatures for 24 h. (c) Optical images showing the flexibility of LPDMS-PES.

rigid perfluorinated layer in resisting crystal adhesion. The highly slippery liquid-like surface layer can provide a unique lubrication effect, and effectively inhibit surface contamination by various matters, ranging from liquids, bio-foulants to solids [21,39]. Therefore, the grafted LPDMS molecular layers should be able to protect the LPDMS-PES membrane from adhering salt crystals formed in the bulk solution. In contrast, the grafted PFOS layer with higher surface friction and adhesion can hardly prevent salt crystals from accumulation, resulting in severe contamination and wetting of the PFOS-PES membrane.

Chemical and thermal stability of the prepared membranes are critical for their practical applications in membrane distillation. To investigate its chemical stability in strong acid or strong alkaline solutions, the LPDMS-PES membrane was immersed in a pH 3 HCl solution or a pH 10 NaOH solution for 2 h. After surface cleaning and drying, the corresponding water contact angles (WCAs) were measured (Fig. 6a). It was found that the change in the WCA of LPDMS-PES was small after either acidic or alkaline solution treatment, indicating the maintenance of good hydrophobicity and suitable WCA values for MD applications after chemical exposure. To assess the thermal stability, LPDMS-PES was subjected to ovens at temperatures of 110, 120, 130, and 140 °C for 24 h, followed by WCA measurements. The results demonstrated negligible changes in the contact angle (Fig. 6b), revealing its excellent thermal stability. Additionally, LPDMS-PES exhibited decent durability against mechanical bending, without cracking even after undergoing hundreds of bending cycles (Fig. 6c).

In conclusion, an environmentally friendly non-fluorinated liquid-like membrane LPDMS-PES was developed for effective membrane distillation in this study. It should be mentioned that the PES polymer has a low and comparable thermal conductivity (0.13–0.18 W m^{-1} K^{-1}) to the PVDF (0.14–0.20 W m^{-1} K^{-1}) and PTFE (0.17–0.30 W m^{-1} K^{-1}) polymers [44] commonly used in traditional MD membranes, and the very thin nanoscale surface coating has little effect on the thermal conductivity. The resulting LPDMS-PES is thus expected to have a low heat transfer efficiency, which is desirable for MD applications. Notably, LPDMS-PES demonstrated a drastically enhanced scale resistance compared to the perfluorinated membrane PFOS-PES in both heterogeneous nucleation-dominated and crystal deposition-dominated scaling tests. The excellent anti-scaling ability of LPDMS-PES should be attributed to the nucleation inhibition ability of the dynamic liquid-like LPDMS brushes and their low adhesion characteristics. Consequently, LPDMS-PES was able to significantly delaying membrane wetting in continuous membrane distillation processes. Additionally, LPDMS-PES exhibited excellent chemical and thermal stability, and hold great promise for water desalination. Our findings not only provide a facile and environmentally friendly alternative to conventional fluorine-containing membranes for membrane distillation, but also offer a highly-effective strategy to address the challenge of scaling issues in membrane separation.

Declaration of competing interest

The authors declare that they have no known competing financial interests or personal relationships that could have appeared to influence the work reported in this paper.

Acknowledgments

This work is supported by National Natural Science Foundation of China (Nos. 22072185, 12072381), Guangdong Basic and Applied Basic Research Foundation (No. 2021A1515110221) and Fundamental Research Funds for the Central Universities, Sun Yat-sen University (No. 23yxqntd002).

Supplementary materials

Supplementary material associated with this article can be found, in the online version, at doi:10.1016/j.cclet.2024.109883.

References

[1] S. Xie, Z. Li, N.H. Wong, et al., J. Membr. Sci. 648 (2022) 120297.
[2] Y. He, Y. Zhang, F. Liang, et al., J. Membr. Sci. 672 (2023) 121444.
[3] H. Zhai, R. Qu, X. Li, et al., ACS Appl. Mater. Interfaces 13 (2021) 48171–48178.
[4] X. Mao, J. Shen, Y. Shen, et al., Chem. Eng. J. 456 (2023) 141144.
[5] K. Yuan, Y. Liu, H. Feng, et al., Chin. Chem. Lett. 35 (2024) 109022.
[6] H. Zhang, L. Li, L. Geng, et al., Chemosphere 311 (2023) 137163.
[7] T. Ni, J. Lin, L. Kong, S. Zhao, Chin. Chem. Lett. 32 (2021) 3298–3306.
[8] Z. Xiong, Q. Lai, J. Lu, et al., J. Membr. Sci. 674 (2023) 121546.
[9] S. Zhao, P.H.M. Feron, X. Chen, et al., Desalination 552 (2023) 116434.
[10] T. Horseman, Y. Yin, K.S.S. Christie, et al., ACS ES&T Engg 1 (2021) 117–140.
[11] M. Huang, J. Song, Q. Deng, et al., Desalination 527 (2022) 115563.
[12] W. Zhang, Y. Li, J. Liu, et al., J. Membr. Sci. 535 (2017) 258–267.
[13] K.S.S. Christie, T. Horseman, R. Wang, et al., Desalination 525 (2022) 115499.
[14] X. Liao, S. Chou, C. Gu, et al., J. Membr. Sci. 665 (2023) 121130.
[15] X. Liao, P. Dai, Y. Wang, et al., J. Membr. Sci. 650 (2022) 120423.
[16] C. Ji, Z. Zhu, L. Zhong, et al., Desalination 519 (2021) 115185.
[17] Z. Wei, Y. Jin, J. Li, et al., Desalination 529 (2022) 115649.
[18] G.R. Xu, M. Wang, K. Xu, et al., Desalination 565 (2023) 116833.
[19] A.L. McGaughey, P. Karandikar, M. Gupta, A.E. Childress, ACS Appl, Polym. Mater. 2 (2020) 1256–1267.
[20] X. Li, J. Yan, T. Yu, B. Zhang, Colloids Surf. A: Physicochem. Eng. Asp. 642 (2022) 128701.
[21] L. Chen, S. Huang, R.H.A. Ras, X. Tian, Nat. Rev. Chem. 7 (2023) 123–137.
[22] L. Wang, T.J. McCarthy, Angew. Chem. Int. Ed. 55 (2016) 244–248.
[23] Y.X. Huang, D.Q. Liang, C.H. Luo, et al., J. Membr. Sci. 637 (2021) 119673.
[24] L. Chen, Q. Feng, S. Huang, et al., J. Membr. Sci. 610 (2020) 118240.
[25] E.J. Lee, B.J. Deka, J. Guo, et al., Environ. Sci. Technol. 51 (2017) 10117–10126.
[26] A.A. Khan, M.I. Siyal, C.K. Lee, et al., Sep. Purif. Technol. 210 (2019) 20–28.
[27] D. Liu, J. Cao, M. Qiu, et al., Sep. Purif. Technol. 295 (2022) 121282.
[28] H. Shan, J. Liu, X. Li, et al., J. Membr. Sci. 567 (2018) 166–180.
[29] Y. Chen, X. Yu, L. Chen, et al., Environ. Sci. Technol. 55 (2021) 8839–8847.
[30] S.M. Kang, N.S. Hwang, J. Yeom, et al., Adv. Funct. Mater. 22 (2012) 2949–2955.
[31] D. Gan, W. Xing, L. Jiang, et al., Nat. Commun. 10 (2019) 1487.
[32] A. Quddus, L.M. Al-Hadhrami, J Thermophys Heat Trans 25 (2011) 112–118.
[33] A. Herz, M.R. Malayeri, H. Müller-Steinhagen, Energy Convers. Manag. 49 (2008) 3381–3386.
[34] S. Wooh, D. Vollmer, Angew. Chem. Int. Ed. 55 (2016) 6822–6824.
[35] Z.S. Tai, M.H.A. Aziz, M.H.D. Othman, et al., Chapter 8 - An overview of membrane distillation, in: A.F. Ismail, M.A. Rahman, M.H.D. Othman, T. Matsuura (Eds.), Membrane Separation Principles and Applications, Elsevier, 2019, pp. 251–281.

[36] S. Shirazi, C.J. Lin, D. Chen, Desalination 250 (2010) 236–248.
[37] E. Curcio, E. Fontananova, G. Di Profio, E. Drioli, J. Phys. Chem. B 110 (2006) 12438–12445.
[38] D.M. Warsinger, A. Servi, S. Van Belleghem, et al., J. Membr. Sci. 505 (2016) 241–252.
[39] P. Liu, H. Zhang, W. He, et al., ACS Nano 11 (2017) 2248–2256.
[40] Z. Xiao, Z. Li, H. Guo, et al., Desalination 466 (2019) 36–43.
[41] Z. Xiao, R. Zheng, Y. Liu, et al., Water Res. 155 (2019) 152–161.
[42] S. Huang, J. Li, L. Liu, et al., Adv. Mater. 31 (2019) 1901417.
[43] J.W. Krumpfer, T.J. McCarthy, Faraday Discuss. 146 (2010) 103–111.
[44] Y. Yang, Thermal conductivity, in: J.E. Mark (Ed.), Physical Properties of Polymers Handbook, Springer, New York, 2007, pp. 155–163.